Nanoscale

Accepted Manuscript

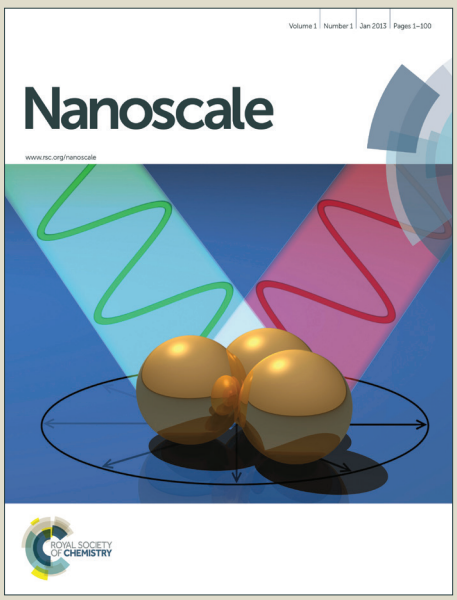

ROYAL SOCIETY OF CHEMISTRY

www.rsc.org/nanoscale

Cite this: DOI: 10.1039/c0xx00000x

www.rsc.org/jmcc

PAPER

Hybrid inverse opals for regulating cell adhesion and orientation

Jie Lu,[a] Fuyin Zheng,[a] Yao Cheng,[a] Haibo Ding,[a] Yuanjin Zhao[*a,b], Zhongze Gu[*a,b]

Received (in XXX, XXX) Xth XXXXXXXXX 20XX, Accepted Xth XXXXXXXXX 20XX
DOI: 10.1039/b000000x

Cell adhesion and alignment are two important considerations in tissue engineering applications as they can regulate the subsequent cell proliferation activity and differentiation program. Although many effects have been applied to regulate the adhesion or alignment of cells by using physical and chemical methods, it is still a challenge to regulate these cell behaviors simultaneously. Here, we present novel substrates with tunable nanoscale patterned structures for regulating the adhesion and alignment of cells. The substrates with different degrees of pattern orientation were achieved by customizing the amount of stretching applied to polymer inverse opal films. Cells cultured on these substrates showed adjustable morphology and alignment. Moreover, soft hydrogels, which have poor plasticity and are difficult to cast into patterned structures, were applied to infiltrate the inverse opal structure. We demonstrated that the adhesion ratio of cells could be regulated by these hybrid substrates, as well as adjusting the cell morphology and alignment. These features of functional inverse opal substrates make them suitable for important applications in tissue engineering.

Introduction

Cell adhesion and alignment play an important role during embryonic development, proliferation, differentiation, wound healing, and even pathological processes.[1] Generally, the adhesion of cells is related to the chemical properties of the substrate surface on which the cell is located.[2] Inspired by biology, the surfaces of substrates have been modified with a series of biological molecules, such as arginine-glycine-aspartate peptides, fibronectin, laminin, collagen, and other ECM proteins, for improving the adhesion of cells.[3] This behavior has also been studied on the surface of nonbiological molecules, such as synthetic polymers, metals, ceramics, carbon-based materials, and other composite materials.[4] On these surfaces, the adhesion of cells can be regulated by changes to the surface energy, charge, and wettability provided for cell growth.[5] However, such chemical modifications have little influence on the orientation of cells on the substrate surface.

Recently, substrates with specific surface topography patterns have been suggested for regulating cell behaviour.[6] It was found that cells could grow in a certain orientation on substrates patterned with grooves or ridges.[7] A series of strategies were then developed for the fabrication of the patterned substrates. Top-down approaches could be realized by using photolithography, inkjet printing, computer-assisted laser ablation or etching, etc.[8] With these approaches, a wide range of high-quality patterned microstructures has been achieved.[9] However, the high cost, low time efficiency, and some technological limitations of these approaches have restricted their use.[10] In contrast, bottom-up approaches, which take advantage of physicochemical interactions for the hierarchical synthesis of ordered nanostructures through the self-assembly of basic building blocks, are low cost, time effective, and are not restricted by nanoscale dimensions.[11] However, it is still a challenge for bottom-up approaches to construct patterned substrates with ordered grooves or ridges. This, together with the debatable biocompatibility of the substrate materials, has limited their applications in cell culture. Thus, novel substrates for regulating the adhesion and alignment of cells are still anticipated.

In this paper, we present a simple method for fabricating patterned substrates with the desired features for regulating the adhesion and alignment of cells. Our substrate was a stretched inverse opal structure that was derived from the convenient bottom-up approach of the self-assembly of colloidal nanoparticles. The nanoscale-patterned structures with different degrees of orientation were achieved by customizing the amount of stretching experienced by the inverse opal substrates. Cells cultured on the substrates with these patterned structures showed adjustable morphology and alignment. Moreover, a series of soft hydrogels, which have poor plasticity and are difficult to cast into patterned structures, could also be applied to infiltrate the inverse opal structure for cell research applications. It was found that the adhesion ratio of cells could be regulated by the hybrid substrates, as well as adjusting the cell morphology and alignment. We anticipate that such functional inverse opal substrates will have important applications in tissue engineering, especially for tissues with anisotropic structures, such as cardiac muscle, blood vessel, tendon, and ligament

Result and Discussion

Fabrication of the stretched inverse opal substrates

The stretched inverse opal substrates were derived from colloidal

crystal templates (Figure 1a). To obtain the templates, glass slides were inserted vertically into a bottle containing an ethanol solution of monodisperse SiO_2 nanoparticles. After evaporation of the solvent, an array of self-assembled SiO_2 nanoparticles formed on the surface of the slides, as shown in Figures 1b and 1c. The slides with the templates were sintered at 400 °C to enhance the junction structures of the SiO_2 nanoparticles and the mechanical strength of the templates. Then, polystyrene (PS)/toluene solution infiltrated the voids of the colloidal nanoparticle array templates. After heating in an oven to evaporate the solvent and solidify the PS materials, the glass slides and the silica nanoparticle templates were etched with hydrofluoric acid (HF) to form a freestanding PS inverse opal film (Figures 1d and 1e).

The pore size and the scaffold materials of the inverse opal film were thoroughly investigated during fabrication. Typically, the size of animal cells ranges from several microns to tens of microns, and the substrates with a comparable pattern size would have an obvious effect on the cell behavior. Thus, we designed the original pore size of the inverse opal film to range from 500 nm to 1 μm because their surface could form patterned structures of several microns after being stretched. However, the quality of the inverse opal film with a large pore size was poor because the big silica nanoparticles with sizes more than 500 nm were difficult to form into ordered arrays by the vertical deposition method. Considering this to be contradictory, the silica nanoparticles with a diameter around 500 nm were used for generating the templates. For constructing the inverse opal, PS was chosen as the scaffold material because it has adequate mechanical strength for cell culture applications, having been used previously as the raw material for standard petri dishes and multiwell plates in cell culturing. In addition, remolding of the PS materials was easy to realize when the PS was heated to its phase-transition temperature. This imparted the ability to stretch on the PS inverse opal.

Under these conditions, the inverse opal films could be stretched to several times their original length by using a vernier caliper in an 80 °C water bath (Figures 1f and 1h). The microstructures of the inverse opal films stretched to three and six times their length were characterized by a scanning electron microscope (SEM), as shown in Figures 1g and 1i. It was observed that the strain did not damage the continuity of the retained inverse opal PS film. The three-dimensionally ordered nanoscale pore structure of the films changed from round to ellipse during stretching. These elliptical pores displayed a certain degree of orientation along the direction of stretching, which indicated its potential as a useful substrate for regulating cell alignment. Generally, the further that the inverse opal film was stretched, the higher the degree of orientation of the substrate that appeared. However, stretching the film too far would destroy the ordered structure of the elliptical pores on the films, and a stretching ratio of six was the feasible maximum ratio. Therefore, films stretched to three and six times their original length were employed for further research.

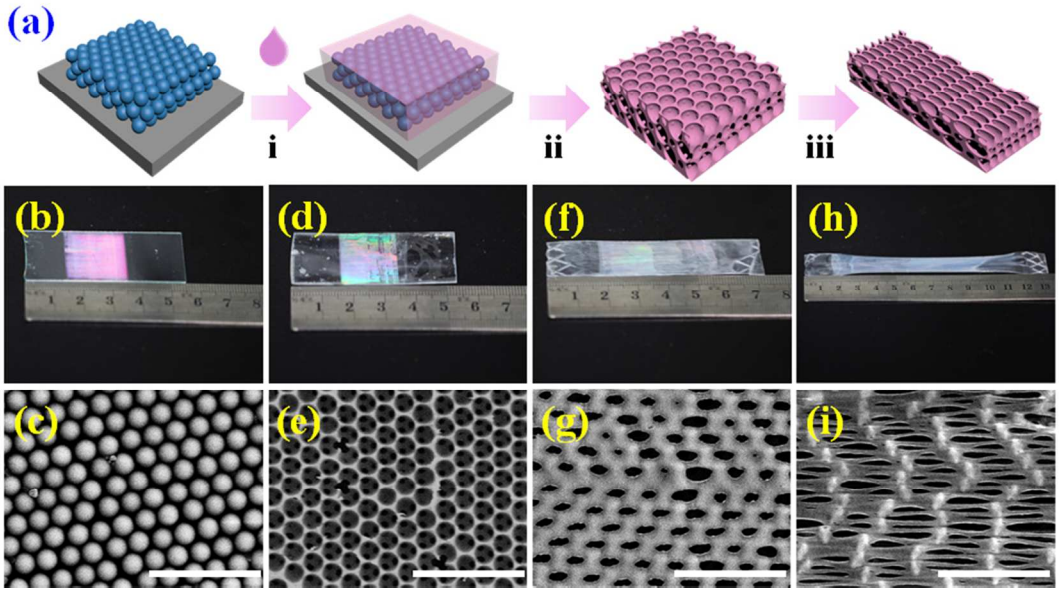

Fig. 1 (a) Schematic diagram of the preparation of the stretched inverse opals; (b-i) photos and SEM images of SiO_2 colloidal crystal template (b, c), inverse opal scaffold (d, e), three times stretched inverse opal scaffold (f, g) and six times stretched inverse opal scaffold (h, i). Scale bars in SEM images are 2μm.

Cell alignment on the stretched substrates

To conduct cell culture research, the stretched inverse opal films were treated with O_2 plasma to increase their hydrophilic properties and encourage cell adhesion. The NIH-3T3 fibroblast was chosen as the typical cell in our study owing to its anisotropic behavior, making the results easy to observe. Figure 2 shows the fluorescent images of the NIH-3T3 fibroblasts cultured for 2 days on different substrate materials, namely, a glass dish, an unstretched inverse opal film, and inverse opal films stretched three and six times their original length. It was found that the cells on the glass dish and the unstretched substrate had disordered microfilaments (Figures 2a and 2b), while the orientation of the cells on the stretched inverse opal substrates became more uniformly aligned as the amount of stretching increased (Figure 2c). In particular, the NIH-3T3 fibroblasts on

the inverse opal substrate stretched to six times the original length spread widely along the direction of stretching and formed tight, closed cell–cell connections (Figure 2d).

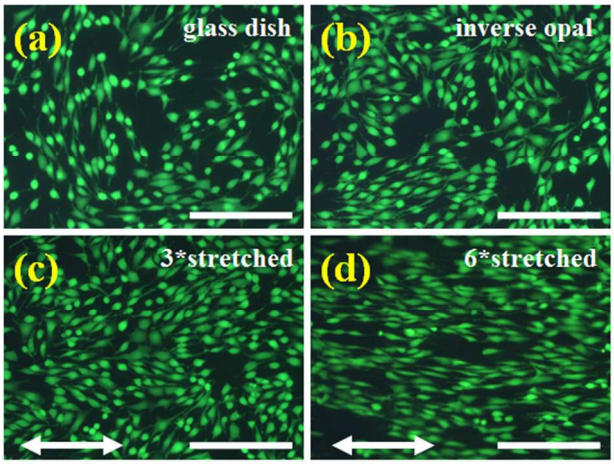

Fig. 2 Fluorescence microscopy images of NIH-3T3 cells cultured on different substrates after 48 hours: (a) on glass dish, (b) on unstretched inverse opal substrate, (c) on three times and (d) six times stretched inverse opal substrates. Scale bars are 200μm. Double-sided arrows indicate the direction of stretching.

The details of the interactions between the NIH-3T3 fibroblasts and the inverse opal scaffolds were characterized by an SEM, as shown in Figure 3. It was found that the cell microfilaments were able to sense the changes associated with an increase in the stretching ratio. The fibroblasts on the glass dishes and unstretched inverse opal substrate showed disordered microfilaments and no specific trend in orientation (Figures 3a–3d), corresponding to their fluorescent images. When the substrate was stretched to three times the original length, the cells showed a high degree of orientation (Figures 3e and 3f). The cell morphology showed a distinct alignment along the stretching direction when the scaffold was stretched to six times the original length, and the microfilaments of the fibroblasts tended to be more elongated in comparison with the other stretched substrates (Figures 3g and 3h).

To gather more information about cell orientation in response to different substrates, we measured and analyzed the angles between the stretching direction and the direction of cell orientation. The ImageJ software (available at http://rsbweb.nih.gov/ij/) was used to analyze the fluorescent images to quantify the cell location relative to the stretching direction. Briefly, the long axis of each cell indicated the direction of cell orientation. The orientation angle values ranged from 0° to 90°. A value of 0° represents an orientation parallel to the stretching direction, whereas 90° represents an orientation perpendicular to the stretching direction (Figure 4a). The percentages of striated cells aligned from 0° to 90° (with incremental interval of 10°) were counted. The results showed that more than 50% of the cells showed an orientation within 10° of parallel to the stretching direction for the inverse opal substrate stretched to six times its length, and this value increased to 90% within 30° to the stretching direction (Figure 4b). In contrast, only approximately 60% and 20% of cells grew within 30° alignment to the stretching direction of the inverse opal substrate stretched to three times its length and the unstretched substrate or glass dish, respectively. These results together with the cell images clearly demonstrated the orientation-induced effects of the stretched substrates on the growing cells.

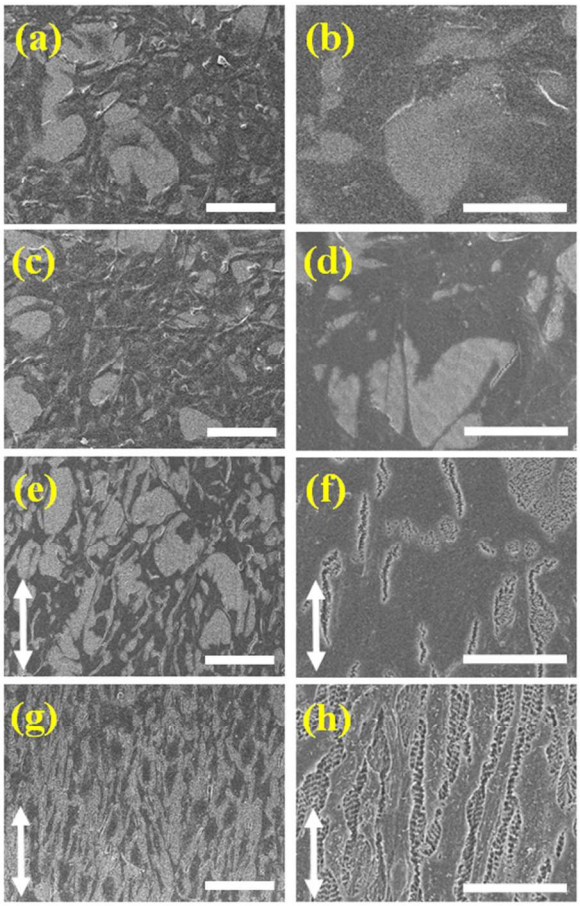

Fig. 3 SEM images of NIH-3T3 cells cultured on different substrates: (a) on glass dish, (b) on unstretched inverse opal substrate, (c) on three times and (d) six times stretched inverse opal substrates. Double-sided arrows indicate the direction of stretching. Scale bars of a, c, e, g and b, d, f, h are 200μm and 20μm respectively. Double-sided arrows indicate the direction of stretching.

Cite this: DOI: 10.1039/c0xx00000x

www.rsc.org/jmcc

PAPER

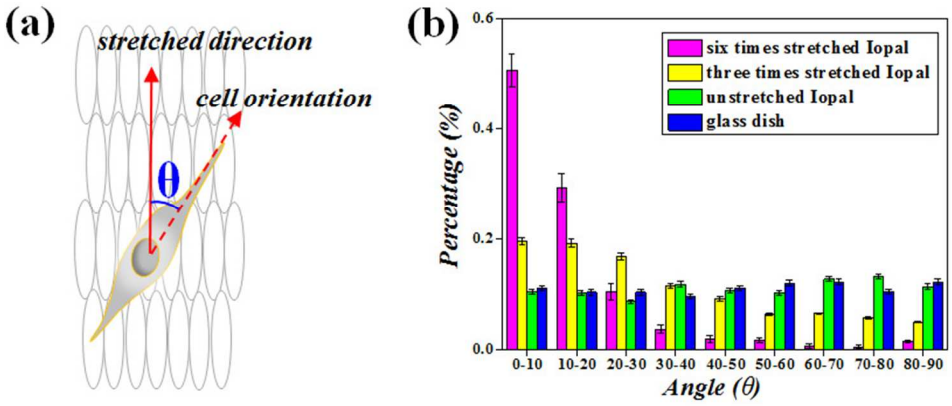

Fig. 4 (a) Schematic diagram of the orientation angle of the cells on the substrates, it is the included angles of the stretched direction and the direction of cell orientation; (b) orientation angle frequency distribution of cells cultured on different substrates after 48 h. 500 cells were measured on each substrate.

Regulation of cell adhesion on the substrates

Although the stretched inverse opal substrates modified the morphology and alignment of the cells, they had less effect on cell adhesion. To provide the substrates with this function, a series of hydrogels were used that could infiltrate the voids of the inverse opal. As different kinds of hydrogels have different affinities to cells, it was anticipated that the hybrid films with these hydrogels in their interstitial voids would have the corresponding affinities to cells. To demonstrate this hypothesis, a high cell-affinity collagen and a low cell-affinity polyethylene glycol (PEG) were selected as model hydrogels to infiltrate the inverse opal structure (Figures 5a–5c) for the cell culture experiments. Figures 5d–5g show the resultant images of the NIH-3T3 fibroblasts cultured on these substrates. As expected, only a small number of cells could be found on the PEG hybrid inverse opal films, while large populations of cells were observed on the collagen hybrid films that were unstretched and stretched six times. In addition, these cells kept their uniform alignment on the stretched hybrid film. These results confirmed the feasibility of our hypothesis.

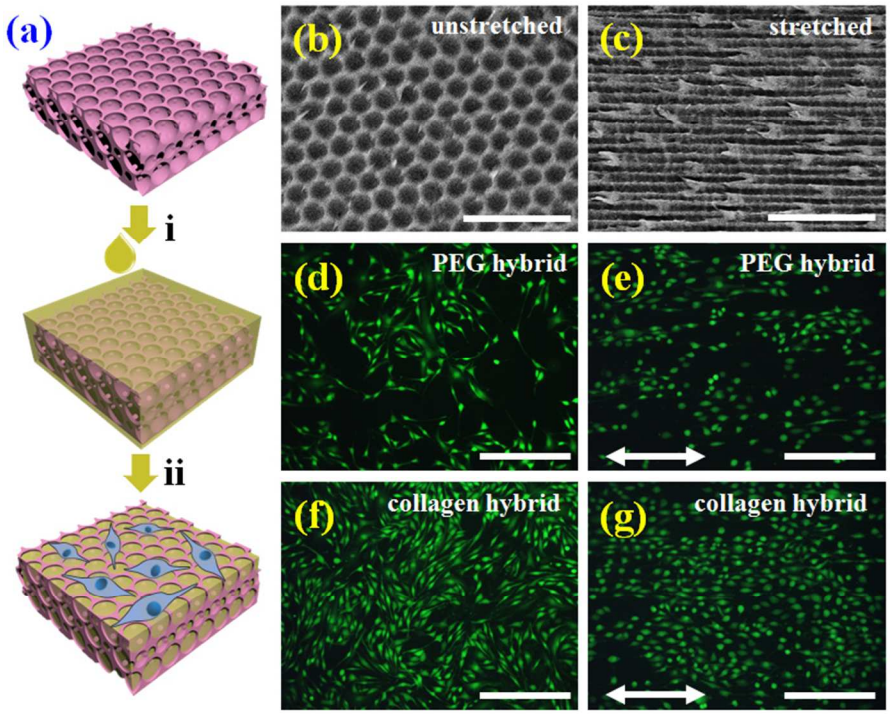

Fig. 5 (a) Schematic diagram of the generation of the hydrogel hybrid inverse opal substrates for cell culturing; (b, c) SEM images of the hydrogel infiltrated inverse opal substrates without and with stretching; (d, e) fluorescence microscopy images of the 3T3 cells cultured on the PEG infiltrated

inverse opal substrates without and with stretching; (f, g) fluorescence microscopy images of 3T3 cells cultured on collagen infiltrated inverse opal substrates without and with stretching. Scale bars of b, c and d–g are 2μm and 100μm respectively. Double-sided arrows indicate the direction of stretching.

The cell viabilities on these materials were also investigated quantitatively by using 3-(4,5-Dimethylthiazol-2-yl)-2,5-diphenyltetrazolium bromide (MTT assays), as presented in Figure 6a. The results indicated that the cell viabilities were highest in the collagen hybrid inverse opal substrate and lowest in the PEG hybrid substrate. These results corresponded with the previous findings from the fluorescent images. The further effect of the different hydrogel hybrid inverse opal substrates on the cell viability was also investigated by counting the numbers of cells after several days of culture, as shown in Figure 6b. It was found that the cells had a fast proliferation capability on the collagen hybrid inverse opal substrate, while the proliferation of the cells on the PEG hybrid substrate was not obvious and their population did not increase after culturing for one week. Thus, the hybrid inverse opal substrate could also have an effect on cell proliferation. All these phenomena indicated the cell behaviors of morphology, orientation, and adhesion could be regulated to a high degree by the stretched hybrid inverse opal substrates.

Besides regulating the cell behaviors, our inverse opal substrates could also be used as a novel platform for the biocompatibility evaluation of different hydrogel materials. To demonstrate this application, a series of soft hydrogels, some of which have poor plasticity and are difficult to cast into patterned structures, were infiltrated into the inverse opal substrates for the cell culture. The biocompatibilities of these soft hydrogel materials were also evaluated from the cell number and the cell viabilities, as indicated in Figure 6. From the result, it was easy to judge the surface biocompatibilities of the hydrogel materials. Their biocompatibilities descending order is collagen, gelatin, arginine-glycine-aspartic (RGD), extracellular matrix (ECM), N-isopropylacrylamide (NIPAM), gelose, silk fibroin and PEG.

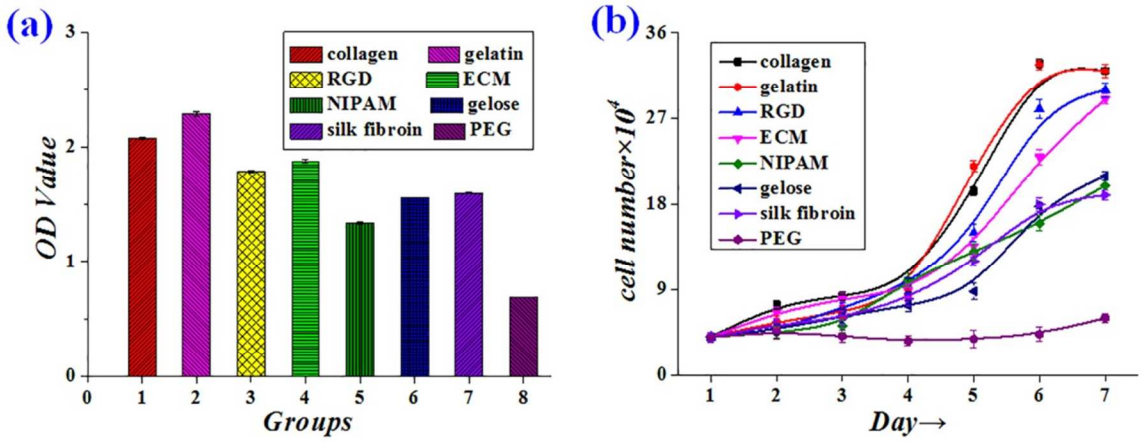

Fig.6 (a) MTT assays of the 3T3 cells cultured on different substrates. Results are presented as mean value ± standard error; n = 3 for the MTT. (b) The viabilities of 3T3 cells cultured on different substrates in one week. The number of replicates at any group was five. Error bars represent standard deviations.

Experimental

Materials

Monodisperse silicon dioxide spheres with diameters of 500 nm were synthesized by State Key Laboratory of Bioelectronics. PBS solution (PH = 7.4) was laboratory homemade. PS, toluene solution, HF and glutaraldehyde were purchased from Aladdin, Shanghai. Fetal bovine serum without Mycoplasma, penicillin-streptomycin double antibiotics, DMEM medium and 0.25% Typin-EDTA was purchased from Gibco, USA. PEG, collagen type I, the photoinitiator, and dimethyl sulfoxide (DMSO) were obtained from Sigma, USA. NIH-3T3 fibroblasts were from Chinese Academy of Sciences. Calcein AM was purchased from molecular prober, USA. MTT (98%) was obtained from J&K Scientific Ltd., Shanghai.

Preparation of inverse opal substrates

Opal film template composed of monodisperse silica spheres was deposited on a glass by vertical deposition. 20% PS/toluene solution was then infiltrated the voids of the opal template. After solidification of the solution, the silica spheres were etched with 4% hydrofluoric acid and washed with demi-water to form a free-standing inverse opal film. Finally, the film was uniaxially stretched to get different degrees at 80 °C by vernier caliper (Masterproof, Germany).

Cell culturing

All the cell culturing substrates required disinfection before cell culture. Inverse opal substrates were firstly immersed in 75% ethanol solution for 5 h. After washing three times with sterile PBS solution and irradiated with ultraviolet light for 3 h, inverse opal substrates were transferred to a 12-well plate (Thermo, USA). Subsequently, NIH-3T3 cells suspension (2×10^3 cells/mL) was added to the substrates. Then, the inverse opal substrates were placed in the incubator (HERA cell 150, Thermo, USA) for 48 h at 37 °C and 5% CO_2.

Fluorescence staining of cells

NIH-3T3 fibroblasts were stained for the visualization of

morphology and alignment by using Calcein-AM. Briefly, cell were washed with PBS twice and incubated with 10μM Calcein-AM solution that diluted with DMSO at 37 ℃ for about 15 minutes. Cells were then washed twice with PBS and stored in PBS, after which stained cells were observed by inverted fluorescence microscope (OLYMPUS IX71, Olympus, Japan).

SEM characterization

The cell-loaded samples were washed three times with PBS and fixed with 2.5% glutaraldehyde solution that diluted with PBS for 6 hours at 4 ℃. The samples were then washed with PBS several times to wash away the glutaraldehyde solution and dehydrated through alcohol of gradient concentrations. The concentration gradient of ethanol is 20%, 40%, 60%, 80% to 100%, and each concentration of ethanol dehydrated the cell sample for 20 min, while dehydrated twice with 100% alcohol to make sure the sample could dehydration completely. After that, the samples were imaged by SEM (S-3000N, Hitachi, Japan) after gold sputter coating.

Preparation of hybrid inverse opal-hydrogel composites

The plasma treated inverse opal substrates were infiltrated thoroughly with solution immediately after it immersed into the per-gel solution of hydrogel. When exposed to some chemical, optical or thermal stimulation, both pre-gel solution inside the nano-pore structure and on the surface of the pore structure could thereafter solidify. Thus, pre-gel solution inner and outside underwent different degree of swelling when immersed into buffer solution due to different porocity in and out of the inverse opal, leading to the rupture between the hydrogel in and out of the pore. Finally we got the hybrid inverse opal-hydrogel composites just after the film stripped from the less swelled hydrogel inside the pore.

Quantitative analysis of cell viability

To carry out MTT assay, the sterile substrates were placed in a 24-well plate (Thermo, USA) separately. The number of cells in each well was 2×10^4. After cell seeding, the 24-well plate was placed in the incubator for 24 h at 37 ℃ and 5% CO_2. Then we transferred the films to a new 24-well plate separately to get rid of the effect of cells adhered on the plate. 360μl new medium and 40μl of MTT solution in PBS were added into each well and incubated at 37 ℃ for 4 h. The culture medium in each well was then removed and 400μl of DMSO was added to completely dissolve the formazan crystals formed in the cells on the films. The absorbance of each well at 490 nm was measured by a microplate reader (Synergy HT, BioTek, USA).

Conclusions

In conclusion, a simple method for fabricating novel patterned substrates for cell culture has been presented. The substrates were stretched polymer inverse opal structures derived from the self-assembly of colloidal nanoparticles. Different orientations of the pattern on the substrates were achieved by customizing the amount of stretch applied to the polymer inverse opal films. Cells cultured on the substrates with these patterned structures showed adjustable morphology and alignment. Moreover, by infiltrating different kinds of soft hydrogels into the stretched inverse opal substrates, the adhesion ratio of cells could also be regulated, as well as adjusting the cell morphology and alignment. These features of the functional stretched inverse opal substrates provide great promise for their use in tissue engineering applications where anisotropic cell distributions are needed.

Acknowledgments

This work was supported by the National Science Foundation of China (Grant Nos. 21105011, 91227124 and 21327902), the National Science Foundation of Jiangsu (Grant No. BK2012735), the research fund for the Doctoral Program of Higher Education of China (20120092130006), the Program for Changjiang Scholars and Innovative Research Team in University (IRT1222), the Technology Invocation Team of Qinglan Project of Jiangsu Province, and the Program for New Century Excellent Talents in University.

Notes and References

[a] *State Key Laboratory of Bioelectronics, Southeast University, Nanjing, 210096, China. E-mail: yjzhao@seu.edu.cn; gu@seu.edu.cn*
[b] *Laboratory of Environment and Biosafety, Research Institute of Southeast University in Suzhou, Suzhou, 215123, China*

1 C. J. Bettinger, R. Langer, J. T. Borenstein, *Angew. Chem., Int. Ed.*, 2009, **48**, 5406; J. H. Huang, J. D. Ding, *Soft Matter*, 2010, **6**, 3395; B. Geiger, J. P. Spatz, A. D. Bershadsky, *Nat. Rev. Mol. Cell. Biol.*, 2009, **10**, 21; S. B. Anderson, C. C. Lin, D. V. Kuntzler, K. S. Anseth, *Biomaterials*, 2011, **32**, 3564; J. W. Xie, M. R. MacEwan, A. G. Schwartz, Y. N. Xia, *Nanoscale*, 2010, **2**, 35.

2 C. S. Chen, M. Mrksich, S. Huang, G. M. Whitesides, D. E. Ingber, *Science*, 1997, **276**, 1425; A. Verma, F. Stellacci, *Small*, 2010 ,**6**, 12; T. Mammoto, D. E. Ingber, *Development*, 2010, **137**, 1407; T. Dvir, B. P. Timko, D. S. Kohane, R. Langer, *Nature Nanotechnology*, 2011, **6**, 13.

3 W. Liu, L. R. Shang, F. Y. Zheng, J. Lu, J. L. Qian, Y. J. Zhao, Z. Z. G, *Small*, 2014, **10**, 8; A. Au, C. A. Boehm, A. M. Mayes, G. F. Muschler, L. G. Griffith, *Biomaterials*, 2007, **28**, 1847; L. Mi, S. Y. Jiang, *Biomaterials*, 2012, **33**, 8928; J. Park, S. Bauer, K. A. Schlegel, F. W. Neukam, K. von der Mark, P. Schmuki, *Small*, 2009, **5**, 666; X. L. Liu, S. T. Wang, *Chem. Soc. Rev.*, 2014, DOI: 10.1039/c3cs60419e.

4 C. M. Kirschner, K. S. Anseth, *Small*, 2013, **9**, 578; D. Kohler, M. Schneider, M. Krüger, C. M. Lehr, H. Möhwald, D. Y. Wang, *Adv. Mater.*, 2011, **23**, 1376; R. Yang, Y. Zhang, J. Y. Li, Q. S. Han, W. Zhang, C. Lu, Y. L. Yang, H. W. Dong, C. Wang, *Nanoscale*, 2013, **5**, 11019; R. Tang, D. F. Moyano, C. Subramani, B. Yan, E. Jeoung, G. Y. Tonga, B. Duncan, Y. Yeh, Z. W. Jiang, C. Kim, V. M. Rotello, *Adv. Mater.*, 2014, DOI: 10.1002/adma.201306030.

5 H. Li, J. X. Wang, Z. L. Pan, L. Y. Cui, L. Xu, R. M. Wang, Y. L. Song, L. Jiang, *J. Mater. Chem.*, 2011, **21**, 1730; X. Yao, Y. L.

Song, L. Jiang, *Adv. Mater.*, 2011, **23**, 719; S. F. Chen, J. Zheng, L. Y. Li, S. Y. Jiang, *J. Am. Chem. Soc*., 2005, **127**, 14473.

6 S. Gerecht, C. J. Bettinger, Z. T. Zhang, J. Borenstein, G. V. Novakovic, R. Langer, *Biomaterials*, 2007, **28**, 4068; Y. C. Wang, Z. M. Tang, Z. Q. Feng, Z. Y. Xie, Z. Z. Gu, *Biomed. Mater*., 2010, **5**, 035011; Y. F. Ding, J. R. Sun, H. W. Ro, Z. Wang, J. Zhou, N. J. Lin, M. T. Cicerone, C. L. Soles, S. L. Gibson, *Adv. Mater*., 2011, **23**, 421; B. Yuan, Y. Jin, Y. Sun, D. Wang, J. Sun, Z. Wang, W. Zhang, X. Jiang, *Adv. Mater.*, 2012, **24**, 890; J. M. Łopacińska, C. Grădinaru, R. Wierzbicki, C. Købler, M. S. Schmidt, M. T. Madsen, M. Skolimowski, M. Dufva, H. Flyvbjerg, K. Mølhave, *Nanoscale*, 2012, **4**, 3739; W. Liu, S. Xing, B. Yuan, W. Zheng, X. Jiang, *Integr. Biol.*, 2013, **5**, 1244; W. Zheng, W. Zhang, X. Jiang, *Adv. Healthcare. Mater.*, 2013, **2**, 95; X. T. Shi, T. Fujie, A. Saito, S. Takeoka, Y. Hou, Y. W. Shu, M. W. Chen, H. K. Wu, A. Khademhosseini, *Adv. Mater*., 2014, DOI: 10.1002/adma.201305804.

7 M. Guvendiren, J. A. Burdick, *Adv. Healthcare Mater*., 2013, **2**, 155; D. H. Kim, K. Han, K. Gupta, K. W. Kwon, K. Y. Suh, A. Levchenko, *Biomaterials*, 2009, **30**, 5433; J. P. Ge, H. Lee, L. He, J. Kim, Z. D. Lu, H. Kim, J. Goebl, S. Kwon, Y. D. Yin, J. *Am. Chem. Soc.*, 2009, **131**, 15687.

8 Z. Liu, H. C. Shum, *Biomicrofluidics*, 2013, **7**, doi: 10.1063/1.4817769.

9 H. Lee, J. Kim, H. Kim, J. Kim, S. Kwon, *Nat. Mater.*, 2010, **9**, 745; H. N. Zhang, J. Shih, J. Zhu, N. A. Kotov, *Nano Lett*., 2012, **12**, 3391.

10 Y. J. Zhao, Z. Y. Xie, H. C. Gu, C. Zhu, Z. Z. Gu, *Chem. Soc. Rev.*, 2012, **41**, 3297.

11 B. F. Ye, H. B. Ding, Y. Cheng, H. C. Gu, Y. J. Zhao, Z. Y. Xie, Z. Z. Gu, *Adv. Mater.*, 2014, DOI: 10.1002/adma.201305035; Z. Y. Xie, L. G. Sun, G. Z. Han, Z. Z. Gu, *Adv. Mater.*, 2008, **20**, 3601–3604; S. W. Choi, J. W. Xie, Y. N. Xia, *Adv. Mater*., 2009, **21**, 2997; Y. W. Liu, C. Leng, B. Chisholm, S. Stafslien, P. Majumdar, Z. Chen, *Langmuir*, 2013, **29**, 2897; L. R. Shang, F. Q. Shangguan, Y. Cheng, J. Lu, Z. Y. Xie, Y. J. Zhao, Z. Z. Gu, *Nanoscale*, 2013, **5**, 9553; Y. S. Xia, T. D. Nguyen, M. Yang, B. Lee, A. Santos, P. Podsiadlo, Z. Y. Tang, S. C. Glotzer, N, A, Kotov, *Nat. Nanotechnol*, 2012, **6**, 580; A. Goyal, C. K. Hall, O. D. Velev, *Soft Matter*, 2010, **6**, 480.